

# NONLINEAR MICRO-MECHANICAL RESPONSE OF THE FIBRE-REINFORCED POLYMER COMPOSITES INCLUDING MATRIX DAMAGE AND FIBRE-MATRIX DECOHESION

\*Zahur Ullah<sup>1</sup>, Łukasz Kaczmarczyk<sup>1</sup> and Chris J. Pearce<sup>1</sup>

<sup>1</sup>School of Engineering, Rankine Building, The University of Glasgow, Glasgow, UK, G12 8LT

\*Zahur.Ullah@glasgow.ac.uk

## ABSTRACT

A three-dimensional multi-scale computational homogenisation framework was developed for the prediction of nonlinear micro-mechanical response of the fibre-reinforced polymer (FRP) composite. Two dominant damage mechanisms, i.e. matrix damage and fibre-matrix decohesion were considered and modelled using a non-associative pressure dependent thermodynamically consistent paraboloidal yield criterion and cohesive elements respectively. A linear-elastic transversely isotropic materials model was used to model yarns within the representative volume element (RVE), the principal directions for which were calculated using a potential flow analysis along these yarns. A unified approach was used to impose the RVE boundary conditions, which allows convenient switching between linear displacement, uniform traction and periodic boundary conditions. Furthermore, the flexibility of hierarchic basis functions and distributed memory parallel programming were fully utilised. The accuracy and performance of the developed computational framework were demonstrated using an RVE with randomly distributed but periodic and axially aligned unidirectional fibres subjected to transverse tension and shear. The macro-strain versus homogenised stress responses were validated against the reference results from the literature. Finally, effects of varying interfacial strength and fracture energy were studied on the homogenised stress versus macro-strain responses.

**Key Words:** *finite element analysis; fibre reinforced polymer; multi-scale computational homogenisation; cohesive zone models; computational plasticity*

## 1. Introduction

As compared to conventional materials, fibre-reinforced polymer (FRP) composites offer exceptional mechanical and chemical properties, making them ideal for a variety of engineering applications, including aerospace, marine, automotive industry, civil structures and prosthetics [1]. On the other hand, their computational modelling is more challenging due to their underlying complicated and heterogeneous microstructure and associated nonlinearities with the matrix damage and fibre-matrix decohesion. Therefore, multi-scale computational homogenisation (CH) provides an accurate modelling framework to simulate the behaviour of FRP composites and determine the macro-scale homogenised (or effective) properties, based on the physics of an underlying, microscopically heterogeneous, representative volume element (RVE). The homogenised properties calculated from the multi-scale CH are subsequently used in the numerical analysis of the macro-level structure.

This paper presents a generalised three-dimensional multi-scale CH framework for prediction of the nonlinear micro-mechanical response of FRP composites, including matrix damage and fibre-matrix decohesion. The pressure dependent thermodynamically consistent paraboloidal yield criterion and cohesive elements are used to model matrix damage and fibres-matrix interfacial decohesion respectively [2, 3], while yarns are considered as linear-elastic and transversely isotropic. The principal directions for the transversely isotropic material model are calculated using a potential flow along these yarns. A unified approach is used to impose the RVE boundary conditions, which allows convenient switching between displacement, traction and periodic boundary conditions [4]. The flexibility of the hierarchic finite element is fully utilised, which permits the use of arbitrary order of approximation leading to accurate results for relatively coarse meshes. Furthermore, the computational framework is designed to take advantage of distributed memory high-performance computing. The developed computational framework is implemented in our group's FE software, MoFEM (Mesh-Oriented Finite Element Method).

## 2. Model components

### 2.1. Material models

The RVE in the case of FRP composites consists of yarns embedded in an epoxy matrix. Epoxy matrix is modelled as an elasto-plastic material using a non-associative pressure dependent thermodynamically consistent paraboloidal yield criterion, the yield surface for which is shown in Figure 1(a) in the principal stress space and is mathematically written as

$$f(\sigma, \sigma_c, \sigma_t) = 6J_2 + 2I_1(\sigma_c - \sigma_t) - 2\sigma_c\sigma_t, \quad (1)$$

where  $\sigma$  is Cauchy stress tensor,  $I_1 = \text{tr}(\sigma)$  is the first invariant of Cauchy stress tensor,  $J_2 = \frac{1}{2}\eta : \eta$  is the second invariant of deviatoric stress  $\eta = \sigma - \frac{1}{3}I_1$  and  $\sigma_t$  and  $\sigma_c$  are yield strengths in tension and compression respectively. A non-associative flow rule is used, for which the plastic potential function is written as

$$g(\sigma, \sigma_c, \sigma_t) = 6J_2 + 2\alpha I_1(\sigma_c - \sigma_t) - 2\sigma_c\sigma_t, \quad \alpha = \frac{1 - 2\nu_p}{1 + \nu_p}, \quad (2)$$

where  $\nu_p$  is a material parameter and is known as plastic Poisson's ratio. Furthermore, the Helmholtz free energy in the case of linear isotropic hardening is written as

$$\psi = \frac{1}{2}\lambda \text{tr}[\boldsymbol{\varepsilon}]^2 + \mu \boldsymbol{\varepsilon} : \boldsymbol{\varepsilon} + \sigma_{t_0}\alpha_0 + \frac{1}{2}H_t\alpha_0^2 + \sigma_{c_0}\alpha_1 + \frac{1}{2}H_c\alpha_1^2, \quad (3)$$

where  $\lambda$  and  $\mu$  are the Lamé parameters,  $\boldsymbol{\varepsilon}$  is the strain tensor,  $\sigma_{t_0}$  and  $\sigma_{c_0}$  are the initial yield strengths in tension and compression respectively,  $\alpha_0$  and  $\alpha_1$  are internal kinematic variables and  $H_t$  and  $H_c$  are hardening parameters in case of tension and compression respectively.

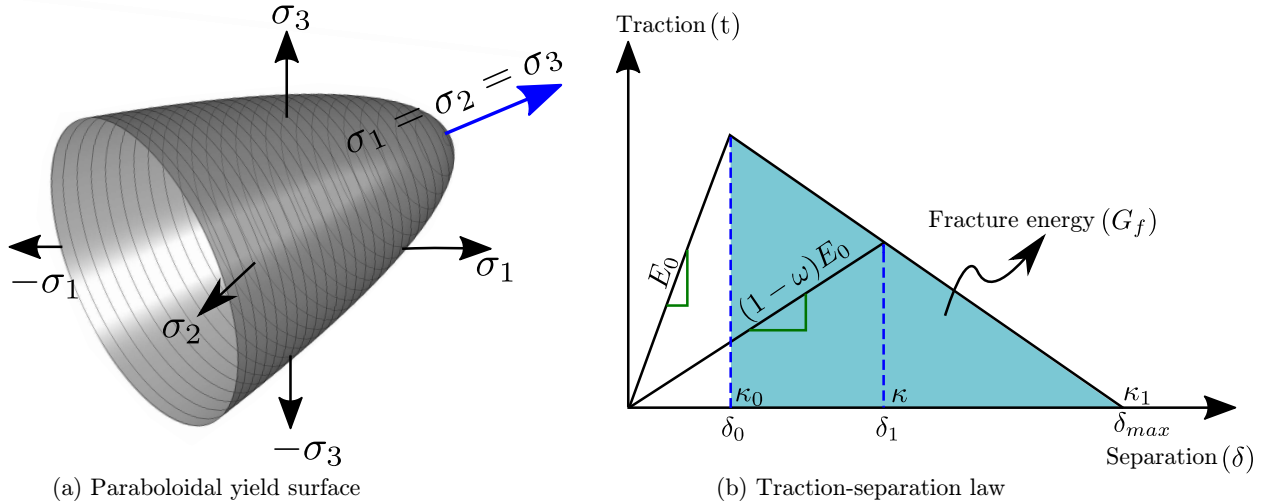


Figure 1: Material models for matrix and fibre-matrix decohesion

Fibre-matrix decohesion is modelled using the standard cohesive elements with a straightforward material model, i.e. linear traction-separation law (shown in Figure 1(b)), which requires only three material parameters including cohesive strength  $f_t$ , fracture energy  $G_f$  and material parameter  $\beta$ , which assign different weight to opening and shear displacements. Mathematically the material model for the cohesive element is written as

$$t = \begin{cases} E_0\delta & \text{if } \delta < \delta_0, \\ (1 - \omega) E_0\delta & \text{if } \delta_0 \leq \delta < \delta_{\max}, \\ 0 & \text{if } \delta \geq \delta_{\max}, \end{cases} \quad (4)$$

where  $E_0$  is the initial stiffness,  $\delta = \sqrt{\delta_n^2 + \beta(\delta_{s1}^2 + \delta_{s2}^2)}$  is displacement jump with  $\delta_n$  and  $\delta_s$  as its normal and shear components and  $\omega$  is damage parameter. Furthermore,  $\kappa$  is a history parameter and is equal to the highest value of displacement jump  $\delta$ .

Finally, yarns are modelled as linear-elastic and transversely-isotropic material. The principal directions for the transversely isotropic material model are determined by solving a potential flow along each yarn [1].

## 2.2. Multi-scale computational homogenisation

In CH, a heterogeneous RVE is associated with each macroscopic Gauss point, the boundary conditions for which are implemented using the generalised procedure proposed in [1, 4]. A small strain formulation is assumed in this paper. For a global step  $n + 1$ , the discretised system of equations in case of an iteration  $i$  of the Newton-Raphson algorithm is written as

$$\begin{bmatrix} \mathbf{K}_{n+1}^i & \mathbf{C}^T \\ \mathbf{C} & \mathbf{0} \end{bmatrix} \begin{Bmatrix} \Delta \mathbf{u}_{n+1}^i \\ \Delta \boldsymbol{\lambda}_{n+1}^i \end{Bmatrix} = \{\mathbf{F}_{n+1}^i\}, \quad (5)$$

where  $\mathbf{K}$  and  $\mathbf{u}$  are the standard FE stiffness matrix and displacement vector respectively and  $\boldsymbol{\lambda}$  is the unknown vector of Lagrange multipliers required to impose the RVE boundary conditions. Matrix  $\mathbf{K}$  consists of contribution of elements from matrix, yarns and yarn-matrix interfaces.  $\mathbf{F}_{n+1}^i$  is a vector of residuals and is written as

$$\mathbf{F}_{n+1}^i = \begin{bmatrix} \mathbf{C}^T \boldsymbol{\lambda}_{n+1}^i - \mathbf{F}_{n+1}^{\text{int}} \\ \mathbf{C} \mathbf{u}_{n+1}^i - \mathbf{D} \bar{\boldsymbol{\varepsilon}}_{n+1} \end{bmatrix}. \quad (6)$$

Matrices  $\mathbf{C}$  and  $\mathbf{D}$  in Equations (5) and (6) are calculated over the boundary  $\Gamma$  of the RVE and are constant throughout the calculations [1, 4]. At Newton-Raphson iteration  $i$ , variable  $\boldsymbol{\phi} = \mathbf{u}, \boldsymbol{\lambda}$  is calculated using  $\boldsymbol{\phi}_{n+1}^i = \boldsymbol{\phi}_n + \sum_{m=1}^i \boldsymbol{\phi}_{n+1}^m$ . In Equation (6),  $\mathbf{F}_{n+1}^{\text{int}}$  is a vector of internal forces consists of contribution of elements from matrix, yarns and yarn-matrix interfaces and  $\bar{\boldsymbol{\varepsilon}}$  is the macro-strain associated with a Gauss point. Furthermore, vectors  $\mathbf{C} \mathbf{u}_{n+1}^i$  and  $\mathbf{C}^T \boldsymbol{\lambda}_{n+1}^i$  are associated with the RVE boundary conditions and are written as

$$\mathbf{C} \mathbf{u}_{n+1}^i = \int_{\Gamma} \mathbf{H} \mathbf{N}^T \mathbf{u}_{n+1}^{hi} d\Gamma, \quad \mathbf{C}^T \boldsymbol{\lambda}_{n+1}^i = \int_{\Gamma} \mathbf{H} \mathbf{N}^T \boldsymbol{\lambda}_{n+1}^{hi} d\Gamma, \quad (7)$$

where  $\mathbf{N}$  is the matrix of shape functions and  $\mathbf{H}$  is a matrix that is specific to the type of boundary conditions used, each row of which represents an admissible distribution of nodal traction forces on the RVE boundary and  $\mathbf{u}^h$  and  $\boldsymbol{\lambda}^h$  are displacements and Lagrange multipliers calculated at a Gauss point, i.e.  $\boldsymbol{\phi}^h = \mathbf{u}^h, \boldsymbol{\lambda}^h = \mathbf{N} \boldsymbol{\phi}^{ei}$ , where  $\boldsymbol{\phi}^e$  is a matrix of displacements or Lagrange multipliers associated with element  $e$ .

## 3. Numerical example

The correct implementation and performance of the computational framework is demonstrated with a polymer composite reinforced with unidirectional fibres subjected to transverse tension and shear. A periodic RVE, consisting of randomly distributed but axially aligned fibres is considered in this case and is shown in Figure 2(a). The RVE is generated using a statistically proven random distribution algorithm proposed in [5] and is consisting of fibres with  $5\mu\text{m}$  diameter and volume fraction of 60%. For the elasto-plastic matrix material Young's modulus, Poisson's ratio, plastic Poisson ratio and initial yield strengths in tension and compression are 3.76 GPa, 0.39, 0.3, 29 MPa and 67 MPa respectively, while for the linear-elastic and isotropic glass fibres, Young's modulus and Poisson's ratio are 74 GPa and 0.2 respectively. For the cohesive elements interface strength and fracture energy are 50 MPa and  $2 \text{ J/m}^2$  respectively. The RVE is discretised with tetrahedral elements including 8,436 and 12,136 elements for matrix and fibres respectively and is shown in Figure 2(b), while the fibres-matrix interfaces are discretised with 1652 zero-thickness cohesive elements. The macro-strain (applied to the RVE by using the periodic boundary conditions) versus the homogenised stress response for both transverse tension and shear cases are compared with the numerical results from [2] and are shown in Figure 2(c), which are in a very good agreement. The final damaged cross-section in the case of transverse-tension is shown in Figure 2(d), where a clear localisation region can be seen. Furthermore, the effect of varying interfacial strength and fracture energy for the transverse tension case is also illustrated in Figure 2(c), which illustrate a more distributed fracture throughout the RVE, e.g. as shown in Figure 2(e).

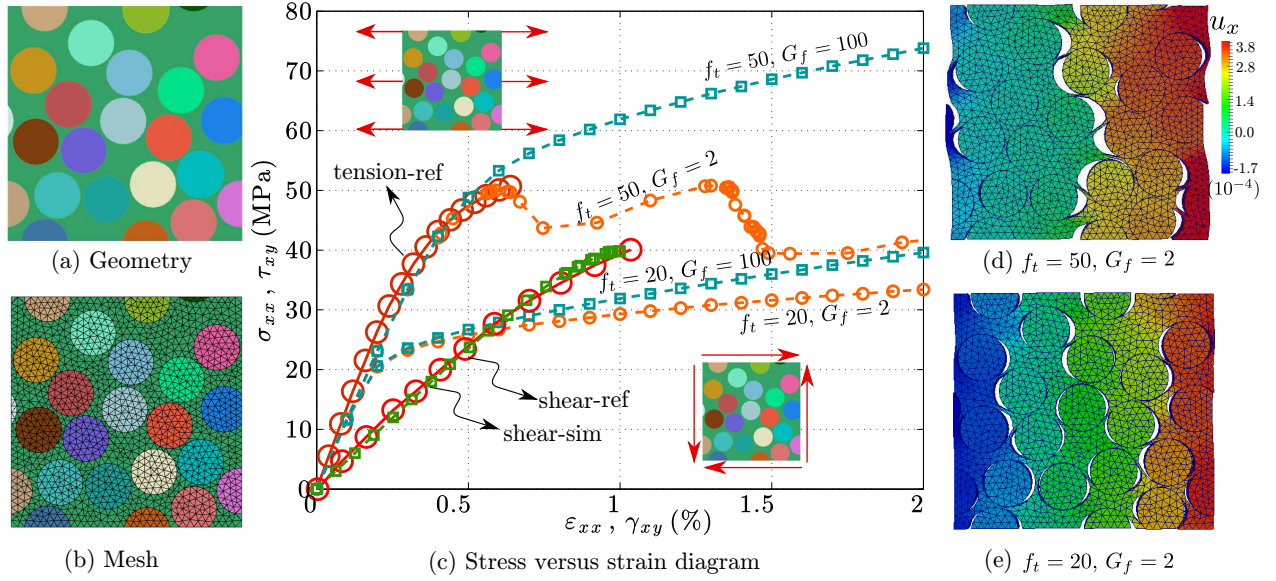


Figure 2: Geometry, mesh, damage and stress-strain plot for the numerical example

#### 4. Conclusions

A three-dimensional, nonlinear micro-mechanical multi-scale computational homogenisation framework is developed for the FRP composites. Matrix and yarns-matrix interfaces are modelled using a paraboloidal yield criterion and cohesive elements respectively, while yarns are considered as linear-elastic and transversely isotropic. The computational framework is validated for FRP composites with unidirectional fibres subjected to transverse tension and shear, the RVE for which are generated using a statistically proven random distribution algorithm. Furthermore, the effect of varying interfacial strength and fracture energy on the homogenised stress versus macro-strain responses is also illustrated.

#### Acknowledgements

The authors gratefully acknowledge the support of the UK Engineering and Physical Sciences Research Council through the Providing Confidence in Durable Composites (DURACOMP) project (Grant Ref.: EP/K026925/1).

#### References

- [1] Z. Ullah, Ł. Kaczmarczyk, S. A. Grammatikos, M. C. Evernden, and C. J. Pearce. Multi-scale computational homogenisation to predict the long-term durability of composite structures. *Computers and Structures (Under Review)*, 2016.
- [2] A. R. Melro, P. P. Camanho, F. M. Andrade Pires, and S. T. Pinho. Micromechanical analysis of polymer composites reinforced by unidirectional fibres: Part II – micromechanical analyses. *International Journal of Solids and Structures*, 50(11–12):1906 – 1915, 2013.
- [3] B. Stier, J. W. Simon, and S. Reese. Comparing experimental results to a numerical meso-scale approach for woven fiber reinforced plastics. *Composite Structures*, 122:553 – 560, 2015.
- [4] Ł. Kaczmarczyk, C. J. Pearce, and N. Bićanić. Scale transition and enforcement of RVE boundary conditions in second-order computational homogenization. *International Journal for Numerical Methods in Engineering*, 74(3):506–522, 2008.
- [5] A. R. Melro, P. P. Camanho, and S. T. Pinho. Generation of random distribution of fibres in long-fibre reinforced composites. *Composites Science and Technology*, 68(9):2092 – 2102, 2008.